Bioorganic & Medicinal Chemistry Letters xxx (2017) xxx–xxx

Contents lists available at ScienceDirect

Bioorganic & Medicinal Chemistry Letters

journal homepage: www.elsevier.com/locate/bmcl

Anti-influenza activity of diazaadamantanes combined with monoterpene moieties

Evgeniy Suslov [a], Vladimir V. Zarubaev [b,*], Alexander V. Slita [b], Konstantin Ponomarev [a], Dina Korchagina [a], Daniel M. Ayine-Tora [c], Jóhannes Reynisson [c], Konstantin Volcho [a,d], Nariman Salakhutdinov [a,d]

[a] Novosibirsk Institute of Organic Chemistry, Siberian Branch of the Russian Academy of Sciences, 630090 Novosibirsk, Russia
[b] Pasteur Institute of Epidemiology and Microbiology, 14 Mira Str., 197101 St. Petersburg, Russia
[c] School of Chemical Sciences, University of Auckland, New Zealand
[d] Novosibirsk State University, Pirogova 2, Novosibirsk 630090, Russian Federation

ARTICLE INFO

Article history:
Received 14 June 2017
Revised 27 August 2017
Accepted 29 August 2017
Available online xxxx

Keywords:
Diaza-adamantane
Terpene
Influenza
Antivirals
Citronellal
Myrtenal

ABSTRACT

The antiviral activity of several diaza-adamantanes containing monoterpenoid moieties against a rimantadine-resistant strain of the influenza A/Puerto Rico/8/34 (H1N1) virus was studied. Hetero-adamantanes containing monoterpene moieties at the aminal position of the heterocycle were found to exhibit lower activity compared to compounds with a diaza-adamantane fragment and a monoterpene moiety linked via an amino group at the 6-position of the hetero-adamantane ring. The highest selectivity index (a ratio of the 50% cytotoxic concentration to the 50% inhibitory concentration) out of 30 was observed for compound **8d**, which contains a citronellal monoterpenoid moiety. Diaza-adamantane **8d** was superior to its adamantane-containing analog **5** both in its anti-influenza activity and selectivity. Furthermore, **8d** has more balanced physicochemical properties than **5**, making the former a more promising drug candidate. Modelling these compounds against an influenza virus M2 ion channel predicted plausible binding modes to both the wild-type and the mutant (S31N).

Influenza is one of the most common infectious diseases known; the infection or its complications cause up to 500,000 deaths every year.[1] The high variability of the influenza virus (aerosol dissemination mechanism, natural reservoirs of its circulation (birds, pigs, etc.), and possibility of interspecific transmission) makes vaccination strategies a challenge, so their effectiveness largely depends on the prediction of strains that will circulate in a given epidemiological season. Its high variability enabled the influenza virus to develop resistance to the few known drugs that are currently used (neuraminidase inhibitors, M2 channel blockers).[2] Thus, developing novel anti-influenza drugs is of a paramount importance.

Some of the first effective low-molecular weight antiviral agents were adamantane derivatives, amantadine **1** and rimantadine **2** (Fig. 1).[3] These compounds exert their antiviral effect by blocking the virus-specific proton channel M2, impairing the virus's ability to enter the cell.[4] However, due to the developed resistance of influenza A virus to adamantyl-containing drugs,[5] *all* of the viral strains (H3N2 and H1N1) isolated in 2009 were *not* susceptible to these drugs.[2] The antiviral activity of adamantane derivatives is known[6–8] to be recovered by introducing substituents on the nitrogen atom. For example, compound **3** with heteroaromatic substituents at the nitrogen atom of 1-amino-adamantane (Fig. 1) exhibited high activity.[9] Furthermore, addition of a hydroxyl on the adamantine scaffold (**4**) resulted in a more drug-like derivative.[9]

Previously, we demonstrated[10] that the introduction of a monoterpenoid moiety to a 1- or 2-amino-adamantane fragment resulted in high activity against the remantadine-resistant influenza virus A(H1N1)pdm09, for compounds containing both acyclic (**5**) and bicyclic (**6**) monoterpenoid moieties (Fig. 1). It should be noted that these compounds are *quite* lipophilic, barring them from *in vivo* experiments.

The insertion of nitrogen atoms into the adamantane core has a significant effect on the physical and chemical properties of the molecule, most notably reducing its lipophilicity.[11,12] We decided to prepare analogs of compounds **5** and **6** that contain two nitrogen atoms in the cycle and study their antiviral activity for the first time.

Compounds **7** and **8** were synthesized according to the previously described procedures.[13–15] For this purpose, hexamethylenetetramine **9** was first converted to the intermediate **10**

* Corresponding author.
E-mail address: zarubaev@gmail.com (V.V. Zarubaev).

http://dx.doi.org/10.1016/j.bmcl.2017.08.062
0960-894X/

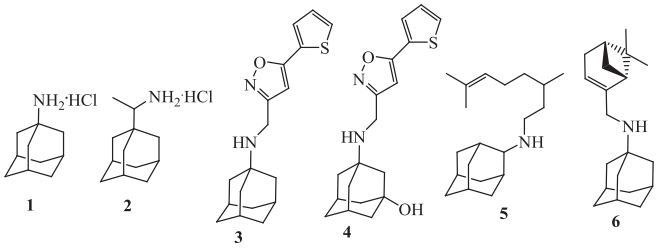

Fig. 1. Structures of adamantane derivatives with anti-influenza activity.

and then to bispidinone hydrochloride **11** (Scheme 1). The interaction between bispidinone **11** and monoterpenoid aldehydes **12a–g** yielded compounds **7a-g**.[16] Monoterpenoids (−)-myrtenal **12a**, citral **12c** (a 1: 1 mixture of *cis*- and *trans*-isomers), citronellal **12d**, and 7-hydroxycitronellal **12e** were commercially available. Ketoaldehyde **12b** was synthesized from monoterpenoid (−)-verbenone via multistep synthesis in accordance with the published procedure.[17] Monocyclic aldehydes **12f** and **12g** were prepared by ozonolysis of (−)-α-pinene according to the previously established reaction pathway[18] and by isomerization of (+)-α-pinene epoxide,[19] respectively.

To produce compounds of the **8** series, compound **10** was used to synthesize oxime **13**, further reduction of which yielded amino-diaza-adamantane **14** (Scheme 1). The reaction of compound **14** with several aldehydes of the monoterpenoid series, followed by the reduction of intermediate imines, led to the target compounds **8a**,**c-e**.[15,20] The **8** derivatives of the **12b**,**f**,**g** aldehydes were not synthesized due to their poor availability.

The synthesized compounds were studied[21] for their antiviral activity against the pandemic influenza virus A/Puerto Rico/8/34 (H1N1) cultivated in cell culture using the procedure described by Sokolov et al.[22] Cytotoxicity of the compounds was evaluated[23] in uninfected MDCK cells as described previously.[24] The obtained data were used to calculate the selectivity index (SI) for each derivative; compounds with SI = 10 and higher were considered as active and the results are presented in Table 1.

Compound **7a**, which contains a bicyclic monoterpene substituent, had no antiviral effect. The introduction of a keto group (**7b**) resulted in a moderate antiviral effect (IC_{50} = 113 μM), low cytotoxicity, and an SI of 8. Interestingly, the same SI and a comparable activity were observed for the reference drug rimantadine **2**. Compounds **7c**,**d** containing citral and citronellal moieties also exhibited moderate activity (IC_{50} of 60–100 μM), but were more toxic than **7b**. The insertion of a hydroxy group into the monoterpene moiety (compound **7e**) led to no anti-antiviral effect. Compounds **7f**,**g** containing monocyclic substituents had no activity.

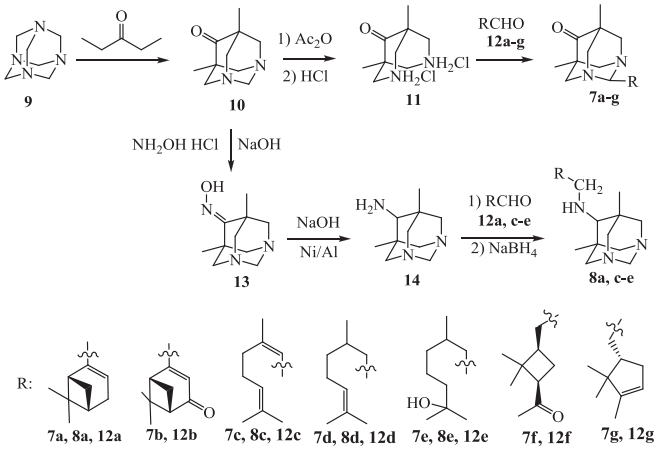

Scheme 1. Synthesis of diazaadamantane derivatives.

Table 1
Antiviral activity and cytotoxicity of compounds **7a–g**, **8a–c**, **e** against influenza virus A/Puerto Rico/8/34 (H1N1) in MDCK cells.

Compound	CC_{50}[a], μM	IC_{50}[b], μM	SI[c]
7a	>1000	>1000	1
7b	907 ± 62	113 ± 15	8
7c	242 ± 18	>99	2
7d	178 ± 11	66 ± 8	3
7e	>904	260 ± 14	3
7f	>943	>943	1
7g	533 ± 36	>331	<2
14	>1823	143 ± 16	13
8a	196 ± 11	64 ± 6	3
8c	>1041	>1041	1
8d	239 ± 21	8 ± 2	30
8e	979 ± 55	134 ± 12	7
Rimantadine	360 ± 21	42 ± 6	8

[a] CC_{50} is the median cytotoxic concentration, i.e. the concentration causing 50% cell death.
[b] IC_{50} is the 50% inhibiting concentration, i.e. the concentration causing 50% decrease of virus replication.
[c] SI is the selectivity index, the CC_{50}/IC_{50} ratio.

For comparison, the antiviral activity of amine **14** (a structural analog of amino-adamantane **1** with known antiviral properties) was tested. It was found to have moderate activity and an SI of 13.

With the addition of a bicyclic monoterpene moiety to compound **14**, resulting in **8a**, a slight increase in the activity was seen, but also with a concomitant increase in cytotoxicity and a decrease in the SI. Compound **8c**, which contains a citral moiety, was completely inactive. However, the citronellal derivative **8d**, which differs from **8c** by the lack of one of the double bonds, exhibited high antiviral activity (IC_{50} of 8 μM) and moderate cytotoxicity, leading to the highest SI of 30. Previously, compound **5** (Fig. 1), a structural analog of **8d** but lacking nitrogen atoms in the cycle, was found to have a SI of 22 with IC_{50} of 18 μM.[10] Therefore, transition from compound **5** to its diaza-adamantane analog **8d** significantly increased both the antiviral activity and the selectivity index. It is worth noting that the introduction of an additional double bond into derivatives of compound **5** led to a tenfold decrease in their activity, as seen here for **8c** and **8d**.[10] Addition of a hydroxy group to the monoterpene moiety (**8e**) caused a sharp decrease in the antiviral activity.

Based on the structures, the M2 channel is the most plausible target for these compounds. The thirteen molecules (**2**, **7a–g**, **8a–c**,**e**, **14**) were docked against an influenza virus M2 protein channel ((PDB ID: 3C9J, resolution 3.5 Å),[25] which was obtained from the Protein Data Bank (PDB).[26,27] The Scigress version FJ 2.6 program[28] was used to prepare the crystal structure for docking, i.e., hydrogen atoms were added and the co-crystallised amantadine (**1**) was removed. The mutant was prepared by changing the Ser31 amino acid residues to Asn31. The configuration of Asn31's side chain was taken from the 5C02 crystal structure of the mutant.[29] The centre of the binding pocket was defined as the nitrogen atom in the amantadine (x = −14.735, y = 14.685, z = −1.856) with a radius of 10 Å. The GoldScore (GS),[30] ChemScore (CS),[31,32] ChemPLP,[33] and Astex statistical potential (ASP)[34] scoring functions were implemented to validate the predicted binding modes and relative energies of the ligands using the GOLD v5.4 software suite.

The M2 protein channel of influenza A virus is a pH dependent channel. It mediates protein-protein dissociation, which takes place during a viral uncoating process when the virus is entrapped in the acidic portion of the lumen of endosomes.[35] This channel is a tetrameric protein bundle with a pore that the anti-influenza drug amantadine targets.[36,37] Due to the high genetic variability of the

Table 2
Criteria of lead-like (LLS), drug-like (DLS) and known drug space (KDS) in terms of molecular descriptors and calculated molecular descriptors of compounds **5** and **8d**.

Molecular descriptors	Criteria of spaces			Compounds	
	LLS	DLS	KDS	**5**	**8d**
Molecular weight (g mol^{-1})	300	500	800	289.5	319.5
Lipophilicity (Log P)	3	5	6.5	5.3	2.9
Hydrogen bond donors (HD)	3	5	7	1.0	1.0
Hydrogen bond acceptors (HA)	3	10	15	1.5	5.5
Polar surface area ($Å^2$) (PSA)	60	140	180	10.3	19.8
Rotatable bonds (RB)	3	10	17	7.0	7.0

influenza virus, most of the current isolates are resistant to the adamantane derivatives. The resistance is mainly conferred by amino acid substitutions in M2 proteins L26F, V27A, S31N and G34E[38,39], S31N being the most important and widely distributed. In our study, the amantadine-resistant virus A/Puerto Rico/8/34 (H1N1) was used with a transmembrane domain sequence 22-SSDPLTIAANIIGILHLTLWILDRL-46 that bears asparagine in position 31.

The modeling shows that the polar diazaadamantane moiety of **8d** occupies the inner portion of the channel where the tetrameric proteins converge, while the bulky substituent occupies the outer wider divergent opening of the channel as shown in Fig. 2A. The binding mode also shows that the side chain carbonyl group of asparagine (Asn31) forms a non-classical hydrogen bond to C–H in the diazaadamantane ring, and the backbone carbonyl oxygen of alanine (Ala30) forms a hydrogen bond with the amine hydrogen on the ligand, as shown in Fig. 2B. This is a plausible binding mode which is consistent with a possible orientation of the amantadine drug molecule, which indicates that bulky groups can be substituted on the amino group of the drug.[25] All the substituted ligands show similar binding modes, though unsubstituted ligands **2** and **14** are oriented in the opposite direction for the wild-type structure. It is worth noting that ligands can flip in this channel, as shown in NMR derived structures.[40] The modelling to the mutated structure gave similar results for the wild-type for GS and CS. The binding scores are similar for all the ligands, including reference compounds **2** and **14** with the exception of ASP giving lower scores for the wild-type structure (see Table S1 in the SI). Interestingly, using ChemPLP, **8d** has the highest score for both wild-type and the mutant. ChemPLP is reported to be the best or one of the best performing scoring functions available.[41,42] Furthermore, **8d** is in second place using CS for both structures and had the best predicted score for the mutant and was in third place for the wild-type using GS, indicating its tight binding to M2.

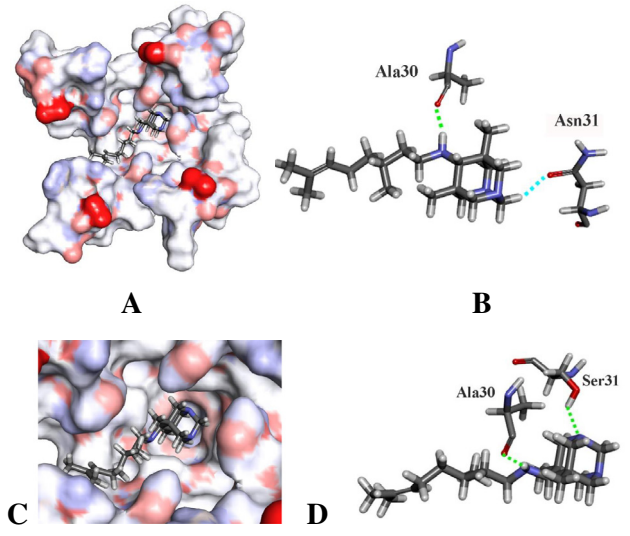

Fig. 2. The docked configuration of **8d** in the binding site of Mutated M2 protein channel as predicted by ChemScore (**A**). The ligand occupies the binding pocket. The protein surface is rendered. Red depicts a negative partial charge on the surface, blue depicts positive partial charge and grey shows neutral/lipophilic areas. (**B**) Hydrogen bond is shown as a green dotted line between **8d** and the amino acid Ala30 whilst non-classical hydrogen bond is shown as a blue dotted line to Asn31. (**C**) Close up of **8d** in the binding pocket. (**D**) Hydrogen bonds are shown as green lines between ligand **8d** and the amino acids Ala30 and Ser31 in the wild-type structure.

As can be seen from the model, **8d** can theoretically bind with both wild-type (S31) and mutated, rimantadine/amantadine resistant (N31) M2. The spectrum of **8d**'s activity will be determined in separate study using a panel of influenza viruses differing in their M2 structure. In addition to M2 inhibition, interaction of **8d** with other viral and/or cellular targets that are unrelated to M2 cannot be ruled out. Further experiments are therefore needed to decipher the specific mode of action of diazaadamantanes against influenza virus, as well as to evaluate their ability to induce viral drug resistance.

Next, the drug-like properties of **5** and its diazaadamantane analogue **8d** were compared. The definitions of lead-like (LLS), drug-like (DLS), and known drug space (KDS) are given in Table 2. The calculated mainstream molecular descriptors of molecular weight (MW), water/octanol partition coefficient (log P), hydrogen bond donors (HD), hydrogen bond acceptors (HA), polar surface area (PSA), and rotatable bonds (RB) for **5** and **8d** are also shown in the Table 2[43]

Both compounds are within the drug-like chemical space, though, notably, **5** is placed in KDS by its predicted log P value of 5.3. Log P is often considered to be the most important molecular descriptor because it is linked to toxicity issues and failure in clinical trials.[44–46] The PSA for the derivatives is quite low, both are in the LLS with **5**, with only half of **8d**'s polar surface area. In all, it can be argued that **8d** conforms well to the DLS whereas **5** is less balanced, with properties in all three defined areas of chemical space. The QikProp 3.2[47] software package was used to calculate the molecular descriptors of the compounds. The reliability of the prediction power of QikProp is established for the molecular descriptors used in this study.[48]

In conclusion, we studied the anti-influenza virus activity of compounds combining hetero-adamantane and monoterpenoid moieties. Although most of the tested compounds showed moderate activity and a low selectivity index, we found that compound **8d** had a high activity against the rimantadine-resistant strain of the influenza A/Puerto Rico/8/34 (H1N1) virus and moderate cytotoxicity, which both led to a very favorable SI of 30. Compound **8d** had much higher activity than both amino-diazaadamantane **14** and its structural analog **5**, without heteroatoms in the adamantane scaffold. Finally, **8d** has excellent drug-like properties, whereas compound **5** is much less balanced. Finally, compound **8d** demonstrated high affinity to an influenza virus M2 protein channel, based on the molecular modelling results.

Please cite this article in press as: Suslov E., et al. Bioorg. Med. Chem. Lett. (2017), http://dx.doi.org/10.1016/j.bmcl.2017.08.062

Acknowledgments

This work was supported by Russian Scientific Foundation (grant 15-13-00017). Spectral and analytical investigations were carried out at Collective Chemical Service Center of Siberian Branch of the Russian Academy of Sciences.

A. Supplementary data

Supplementary data associated with this article can be found, in the online version, at http://dx.doi.org/10.1016/j.bmcl.2017.08.062.

References

1. Cianci C, Gerritz SW, Deminie C, Krystal M. Influenza nucleoprotein: promising target for antiviral chemotherapy. *Antiviral Chem Chemother*. 2013;23:77–91.
2. Fiore AE, Fry A, Shay D, Gubareva L, Bresee JS, Uyeki TM. Antiviral agents for the treatment and chemoprophylaxis of influenza. *MMWR Recomm Rep*. 2011;60:1–24.
3. Wanka L, Iqbal K, Schreiner PR. The lipophilic bullet hits the targets: medicinal chemistry of adamantane derivatives. *Chem Rev*. 2013;113:3516–3604.
4. Schnell JR, Chou JJ. Structure and mechanism of the M2 proton channel of influenza A virus. *Nature*. 2008;451:591–596.
5. Dong G, Peng C, Luo J, et al. Adamantane-resistant influenza a viruses in the world (1902–2013): frequency and distribution of M2 gene mutations. *PLoS One*. 2015;10:e0119115.
6. Shen Z, Lou K, Wang W. New small-molecule drug design strategies for fighting resistant influenza A. *Acta Pharmaceut Sin B*. 2015;5:419–430.
7. Wang J, Ma C, Wang J, et al. Discovery of novel dual inhibitors of the wild-type and the most prevalent drug-resistant mutant, S31N, of the M2 proton channel from influenza A virus. *J Med Chem*. 2013;56:2804–2812.
8. Li F, Hu Y, Wang Y, Ma C, Wang J. Expeditious lead optimization of isoxazole-containing influenza A virus M2–S31N inhibitors using the Suzuki–Miyaura cross-coupling reaction. *J Med Chem*. 2017;60:1580–1590.
9. Li F, Ma C, DeGrado WF, Wang J. Discovery of highly potent inhibitors targeting the predominant drug-resistant S31N mutant of the influenza A virus M2 proton channel. *J Med Chem*. 2016;59:1207–1216.
10. Teplov GV, Suslov EV, Zarubaev VV, et al. Synthesis of new compounds combining adamantanamine and monoterpene fragments and their antiviral activity against influenza virus A(H1N1)pdm09. *Lett Drug Des Discovery*. 2013;10:477–485.
11. Kuznetsov AI, Zefirov NS. Azaadamantanes with nitrogen atoms in the bridgehead positions. *Russ Chem Rev*. 1989;58:1033–1047.
12. Jimenez-Cruz F, Rios-Olivares H, Gutierrez JLG. Molecular structure of 1-azaadamantanes and 1,3-diazaadamantanes. In: Iriepa I, ed. *Structural analysis of cyclic systems*. Trivandrum: Research Signpost; 2005:101–125.
13. Ponomarev K, Suslov E, Pavlova A, et al. Synthesis and analgesic activity of new compounds combining azaadamantane and monoterpene moieties. *Med Chem Res*. 2015;24:4146–4156.
14. Zakharenko AL, Ponomarev KU, Suslov EV, et al. Inhibitory properties of nitrogen-containing adamantane derivatives with monoterpenoid fragments against tyrosyl-DNA phosphodiesterase 1. *Russ J Bioorg Chem*. 2015;41:657–662.
15. Ponomarev K, Morozova E, Pavlova A, Suslov E, Korchagina D, Nefedov A, Tolstikova T, Volcho K, Salakhutdinov N. Synthesis and analgesic activity of amines combining azaadamantane and monoterpene fragments. *Med Chem*. 2017 [in press].
16. Synthesis of compounds 7a-g: general procedure. To the methanolic solution of hydrochloride 11 (0.1 mmol, 2 mL) an equimolar amount of aldehyde 12a–g and triethylamine (2.5 equivalents) was added. After completion of the reaction (control by gas chromatography), the solvent was distilled off, and the residue was separated on a SiO2 column.
17. Ardashov OV, Demidova YS, Korchagina DV, Simakova IL, Volcho KP, Salakhutdinov NF. The first synthesis of (4*S*,5*R*,6*R*)-5,6-dihydroxy-4-(prop-1-en-2-yl)cyclohex-1-enecarboxylic acid. *Helv Chim Acta*. 2015;98:1442–1455.
18. Barton DHR, Fontana G. Radical chemistry based on (+)-cis-pinononic and (+)-pinonic acids. *Synth Commun*. 1996;26:1953–1968.
19. Lopez L, Mele G, Fiandanes V, Cardellicchio C, Nacci A. Aminium salts catalyzed rearrangement of α-pinene and β-ionone oxides. *Tetrahedron*. 1994;50:9097–9106.
20. Synthesis of compounds 8a, c-e: general procedure. To the methanolic solution of amine 14 (0.1 mmol, 4 mL MeOH) an equimolar amount of aldehyde 12a, c-e was added. The mixture was stirred for 4 hours. Then NaBH4 (0.6 mmol) was added. After addition of the NaBH4 to the reaction mixture, it was stirred for ~1.5 h. The solvent was distilled off, 8 ml of saturated NaCl solution was added to the residue in the flask. The product was extracted with Et2O. Isolation of amines 8a, c-e from the reaction mixture was accomplished by precipitation from solution in ether in the form of hydrochloric salts by adding ethylacetate saturated with hydrogen chloride. The precipitate was filtered off, washed with ether and treated with saturated sodium bicarbonate solution. The product was extracted from the aqueous solution by ether. The organic phase was dried over Na2SO4. Then drying agent was filtered off, and the solvent was distilled off on a rotary evaporator.
21. The compounds in appropriate concentrations were dissolved in 0.1 ml DMSO and final solutions were prepared by adding MEM with 1 μg/ml trypsin. Compounds were incubated with MDCK cells for 1 h at 36 °C. Each concentration of the compounds was tested in triplicate. The cell culture was then infected with influenza virus A/Puerto Rico/8/34 (H1N1) (moi 0.01) for 24 h at 36 °C in the presence of 5% CO2. A virus titer in the supernatant was determined by hemagglutination test after cultivating of the virus progeny in MDCK cells for 48 h at 36 °C in the presence of 5% CO2. The 50% inhibiting concentrations (IC50) and the selectivity index (SI, the ratio of CC50 to IC50) were calculated from the data obtained.
22. Sokolov DN, Zarubaev VV, Shtro AA, et al. Anti-viral activity of (−)- and (+)-usnic acids and their derivatives against influenza virus A(H1N1)2009. *Bioorg Med Chem Lett*. 2012;22:7060–7064.
23. The microtetrazolium test (MTT) was used to study the cytotoxicity of the compounds. Briefly, a series of three-fold dilutions of each compound in MEM were prepared. MDCK cells were incubated for 48 h at 36°C in 5% CO2 in the presence of the dissolved substances. The cells were washed twice with phosphate-buffered saline (PBS), and a solution of 3-(4,5-dimethylthiazolyl-2) 2,5-diphenyltetrazolium bromide (ICN Biochemicals Inc., Aurora, Ohio) (0.5 μg/ml) in PBS was added to the wells. After 1h incubation, the wells were washed and the formazan residue was dissolved in DMSO (0.1 ml per well). The optical density of cells was then measured on a Victor 2 1440 multifunctional reader (Perkin Elmer, Finland) at wavelength of 535 nm and plotted against the concentration of compounds. Each concentration was tested in three parallels. The 50% cytotoxic concentration (CC50) of each compound was calculated from the data obtained.
24. Mosmann T. Rapid colorimetric assay for cellular growth and survival: application to proliferation and cytotoxicity assays. *J Immunol Methods*. 1983;65:55–63.
25. Stouffer AL, Acharya R, Salom D, et al. Structural basis for the function and inhibition of an influenza virus proton channel. *Nature*. 2008;451:596–599.
26. Berman HM, Westbrook J, Feng J, et al. The protein data bank. *Nucleic Acids Res*. 2000;28:235–242.
27. Berman H, Henrick K, Nakamura H. Announcing the worldwide protein data bank. *Nat Struct Mol Biol*. 2003;10. 980–980.
28. Scigress: Version FJ 2.6 (EU 3.1.7), Fijitsu Limited, 2008–2016.
29. Thomaston JL, DeGrado WF. Crystal structure of the drug-resistant S31N influenza M2 proton channel. *Protein Sci*. 2016;25:1551–1554.
30. Jones G, Willett P, Glen RC, Leach AR, Taylor R. Development and validation of a genetic algorithm for flexible docking. *J Mol Biol*. 1997;267:727–748.
31. Eldridge MD, Murray CW, Auton TR, Paolini GV, Mee RP. Empirical scoring functions: I. The development of a fast empirical scoring function to estimate the binding affinity of ligands in receptor complexes. *J Comput-Aided Mol Des*. 1997;11:425–445.
32. Verdonk ML, Cole JC, Hartshorn MJ, Murray CW, Taylor RD. Improved protein-ligand docking using GOLD. *Proteins*. 2003;52:609–623.
33. Korb O, Stutzle T, Exner TE. Empirical scoring functions for advanced protein-ligand docking with PLANTS. *J Chem Inf Model*. 2009;49:84–96.
34. Mooij W, Verdonk ML. General and targeted statistical potentials for protein–ligand interactions. *Proteins*. 2005;61:272–287.
35. Mould JA, Drury JE, Frings SM, et al. Permeation and activation of the M_2 ion channel of influenza A virus. *J Biol Chem*. 2000;275:31038–31050.
36. Sakaguchi T, Tu Q, Pinto LH, Lamb RA. The active oligomeric state of the minimalistic influenza virus M2 ion channel is a tetramer. *Proc Natl Acad Sci*. 1997;94:5000–5005.
37. Kovacs FA, Cross TA. Transmembrane four-helix bundle of influenza A M_2 protein channel: structural implications from helix tilt and orientation. *Biophys J*. 1997;73:2511–2517.
38. Furuse Y, Suzuki A, Oshitani H. Large-scale sequence analysis of M gene of influenza A viruses from different species: mechanisms for emergence and spread of amantadine resistance. *Antimicrob Agents Chemother*. 2009;53:4457–4463.
39. Abed Y, Goyette N, Boivin G. Generation and characterization of recombinant influenza A (H1N1) viruses harboring amantadine resistance mutations. *Antimicrob Agents Chemother*. 2005;49:556–559.
40. Wu Y, Canturk B, Jo H, et al. Flipping in the pore: discovery of Inhibitors that bind in different orientations to the Wild-Type versus the Amantadine-Resistant S31N Mutant of Influenza A Virus M_2 Proton Channel. *J Am Chem Soc*. 2014;136:17987–17995.
41. Liebeschuetz JW, Cole JC, Korb O. Pose prediction and virtual screening performance of GOLD scoring functions in a standardized test. *J Comput Aided Mol Des*. 2012;26:737–748.
42. Li Y, Han L, Liu Z, Wang R. Comparative assessment of scoring functions on an updated benchmark: 2. Evaluation methods and general results. *J Chem Inf Mod*. 2014;54:1717–1736.
43. Bade R, Chan H-F, Reynisson J. Characteristics of known drug space. natural products, their derivatives and synthetic drugs. *Eur J Med Chem*. 2010;45:5646–5652.
44. Wenlock MC, Austin RP, Barton P, Davis AM, Leeson PD. A comparison of physiochemical property profiles of development and marketed oral drugs. *J Med Chem*. 2003;46:1250–1256.
45. Hughes JD, Blagg J, Price DA, et al. Physochemical drug properties associated with in vivo toxicological outcomes. *Bioorg Med Chem Lett*. 2008;18:4872–4875.

46. Zhu F, Logan G, Reynisson J. Wine compounds as a source for HTS screening collections. A feasibility study. *Mol Inf.* 2012;31:847–855.
47. QikProp, v3.2; Schrödinger: New York; 2009.
48. Ioakimidis L, Thoukydidis L, Naeem S, Mirza A, Reynisson J. Benchmarking the reliability of QikProp. Correlation between experimental and predicted values. *QSAR Comb Sci.* 2008;27:445–456.